Characterization of PARG Inhibitors and Their Effects on DNA Damage, Repair, and Survival in +/- HRD Cancers

By

Emelia Magro

BS University of Massachusetts – Amherst, 2024

Commented [1]: You do not put your Brown MS information here. Just previous degrees

Thesis

Submitted in partial fulfillment of the requirements for the Degree of Master of Science in the Graduate Program of Biotechnology at Brown University

PROVIDENCE, RHODE ISLAND

May 2026

This thesis by Emelia Magro is accepted in its present form by the Graduate Program in Biotechnology as satisfying the thesis requirements for the degree of Master of Science

Date_____ Signature: _____

Robert W Sobol, PhD, Advisor

Date_____ Signature: _____

Dr. Wynand Roos, PhD, Reader

Date_____ Signature: _____

Dr. Diana Horrigan, PhD, Reader

Commented [2]: Add in this information

Approved by the Graduate Council

Date_____ Signature: _____

David Lindstrom, PhD, Dean of the Graduate School

Commented [3]: Put Dean's name in

Table of Contents

References

Supplemental Figures

Acknowledgements

I would like to sincerely thank my advisor, Robert W. Sobol, for his guidance, support, and mentorship throughout this research. His insight and dedication to the field have been invaluable to my development as a scientist. I am especially grateful to Wynand Roos and Rasha Al Rahahleh for their generous guidance, patience, and expertise. Their mentorship played a critical role in shaping this work, and I deeply appreciate the time they invested in teaching and supporting me. I would also like to thank all members of the Sobol Lab for creating a collaborative and supportive research environment. I am particularly thankful for the master's students in my cohort and the undergraduate researchers, whose teamwork, discussions, and encouragement made this experience both productive and enjoyable.

Finally, I am deeply grateful to my family and friends for their unwavering support, encouragement, and understanding throughout this journey. Their belief in me made this work possible.

Overall Abstract

Ovarian cancer remains a significant clinical gap due to late-stage diagnosis and frequent development of resistance to standard therapies, including platinum-based chemotherapy and PARP inhibitors. Homologous recombination deficiency (HRD) is commonly observed in ovarian cancers which creates vulnerabilities in the DNA damage and repair pathway. Most small molecule inhibitors such as PARPi therapies have been a well-known treatment for ovarian cancers; however, resistance to these current targeted therapies remain a major clinical challenge. Poly (ADP-ribose) glycohydrolase (PARG) inhibition has emerged as a potential strategy to disrupt DNA repair by increasing poly(ADP-ribose) (PAR) accumulation and impairing cellular survival mechanisms.

In this study, we evaluated the effects of multiple different PARGi on PAR accumulation across a panel of ovarian cancer cell lines. Furthermore, we investigated combination treatments such as supplementation of the NAD+ precursor NRH that modulated PAR synthesis to enhance cellular effects of PARG inhibition. In addition, combining PARGi with other DNA damage response (DDR) inhibitors such as PARPi and genotoxic agents were assessed to identify and quantify PAR accumulation and foci formation using confocal microscopy and high-content imaging platforms.

Overall, these studies aim to characterize the impact of PARG inhibition on ovarian cancer cell survival in cancer cell survival and DNA repair signaling. Identifying combination strategies like NRH supplementation may also have an impact on overcoming therapeutic resistance. This study would help to understand differences and significances of inhibition across differenct ovarian

cancer models. These findings may inform the development of a novel treatment approach for ovarian cancers, particular those resistant to current DNA repair-targeted therapies.

Chapter 1: Introduction

Ovarian cancer remains one of the most lethal gynecologic malignancies worldwide, largely due to late-stage diagnosis and the frequent development of resistance to standard therapies. Despite advances in surgery and platinum-based chemotherapy, recurrence occurs in the majority of patients, highlighting the urgent need for new therapeutic strategies that can overcome treatment resistance [1]. Currently, over 225,500 new cases of ovarian cancer are diagnosed each year globally, resulting in about 140,200 deaths attributed to the disease. Specifically in the United States, approximately 22,280 new cases occur annually. Despite continuous improvements in treatments, ovarian cancer mortality has seen minimal improvement in the past ten years. Overall survival for all patients with ovarian cancer is 45.6%, varying greatly based on the stage at diagnosis. At stage I, cancer survival is about 92.1% but decreases to 25% for patients with stage III and IV [2].

The high rate of recurrence and treatment resistance in ovarian cancer has prompted increased investigation into the molecular mechanisms that drive tumor progression and therapeutic response. One pathway that has gained significant attention is the homologous recombination (HR) DNA repair pathway—a high-fidelity pathway responsible for repairing DNA double-strand breaks. Homologous recombination-deficient (HRD) ovarian cancers are quite common and perhaps make up around 65% of ovarian cancers [6, 7]. HRD is frequently observed in ovarian tumors and can arise from mutations or functional alterations in genes involved in

homologous recombination. Among these, mutations in *BRCA1* and *BRCA2* are the most well-characterized and clinically significant. These genes encode proteins that play critical roles in maintaining genomic stability by facilitating DNA repair. When *BRCA* function is lost, cells become unable to effectively repair DNA double-strand breaks through HR, resulting in genomic instability and tumor development [7]. *BRCA* mutational rate in ovarian cancers is about 29% [7].

Current treatments for ovarian cancer have been advancing, particularly platinum-based chemotherapy, neoadjuvant chemotherapy (NACT), and targeted therapies like Poly (ADP-ribose) polymerase (PARP) inhibitors which have improved outcomes for progression-free survival in mutated and HRD-positive patients [8]. However, despite initial responses to chemotherapeutic treatment, many patients develop resistance. Consequently, a large proportion of patients develop recurrent disease that is often more aggressive and therapeutically resistant, contributing significantly to ovarian cancer mortality. Furthermore, over 50% of HRD positive and *BRCA* ovarian cancer patients respond poorly to PARPi therapy highlighting a clinical gap and need for novel therapeutic strategies to overcome chemoresistance in ovarian cancer [9-11].

Poly(ADP-ribose) glycohydrolase (PARG) is the primary enzyme responsible for degrading poly(ADP-ribose) (PAR) chains generated by PAR polymerases. Pharmacologic inhibition of PARG has emerged as tool to probe balance between PAR synthesis and turnover [3]. Here, we evaluated both established and recently reported PARG inhibitors to quantify their effects on cellular PAR accumulation and viability. Because PAR synthesis depends directly on NAD+ pools, we also test these PARG inhibitors in the presence and absence of the NAD+ precursor

NRH to determine whether augmenting NAD+ availability modulates PAR formation and/or cell survival. Together, these experiments will clarify whether enhanced substrate availability (via NRH) amplifies PAR accumulation under PARG blockade [4, 5].

In parallel, we interrogated combination strategies that pair PARG inhibitors with inhibitors of DNA-damage response (DDR) nodes to assess additive or synergistic effects on cell survival. Given that persistent PARylation can interfere with DNA repair signaling and that DDR inhibitors (PARP, DNA-PK, APE-1) exploit specific repair vulnerabilities, combining PARGi with selected DDR agents may reveal mechanistic dependencies and potential synthetic-lethal interactions. Endpoints include quantification of PAR levels and cell viability assays to allow us to map how PARG inhibition reshapes sensitivity to targeted DNA-repair blockade.

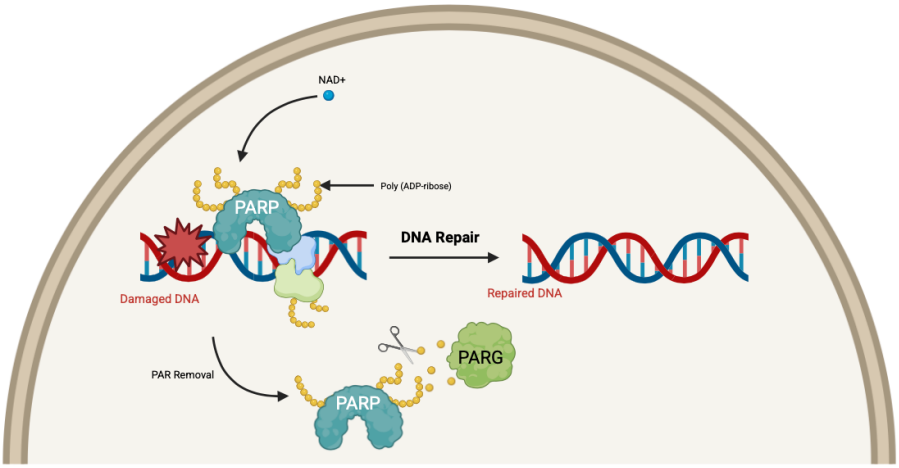

PARG Pathway

Chapter 2: Materials & Methods

Cell and Cell Culture Conditions

Human ovarian cancer cell lines ES-2 (ATCC, Cat# CRL-1978), ES-2/XRCC1-KO (ES-2 cells transfected with purified Cas9 and three gRNA targeting a distinct exon of the XRCC1 gene), ES-2/LivePAR, U2OS/LivePAR which were transformed with a PAR binding domain (PBD), namely the WWE domain of RNF146 (amino acid residues 100-182), fused to EGFP. U2OS cells were obtained from ATCC (Cat# HTB-96). PA-1, COV362, RMUGS, SKOV-3, OVTOKO was provided generously by Dr. Alan D'Andrea (Dana Farber Cancer Institute). All ovarian cell lines were cultured in RPMI 1640 (Corning, Cat# 10-016-CV) supplemented with 10% heat-inactivated fetal bovine serum (Bio-Techne, Cat# S11150H) and 1% penicillin-streptomycin (Thermo Fisher Scientific, Cat# 15140-122). U2OS/LivePAR cells were cultured in D-MEM 10-013CV supplemented with 1% penicillin-streptomycin (Thermo Fisher Scientific, Cat# 15140-122), 10% heat-inactivated fetal bovine serum (Bio-Techne, Cat# S11150H) and 1% L-glutamine (Thermo Fisher Scientific, Cat# 25030-081). All cells were cultured at 37°C with 5% CO2 in 100mm cell culture dishes (Corning, Cat# 08-772-21).

Cells were treated with the following inhibitors: PARG inhibitors PARGi PDD00017273 (Tocris, Cat # 5952), PDD000172738 (Tocris, Cat # 7007), PDD00031705 (Tocris, Cat # 7009) or JA2131 (Sigma, Cat # SML2968-5MG). PARP 1/2 inhibitor ABT-888 (Veliparib; MedChemExpress, Cat# HY-10129) or BMN-673 (Talazoparib; MedChemExpress, Cat# HY-16106). Genotoxins used include N-methyl-N-nitro-N'-nitrosoguanidine (MNNG) (Company and Cat #), Methyl methanesulfonate (MMS), and tert-butyl hydroperoxide (tBuOOH). NRH was a gift from Dr. Marie Migaud (University of South Alabama).

96-Well Viability Analysis

Ovarian cancer cells (105) were seeded in 100mm dishes with 10mL growth medium. At 80% confluency, cells were isolated by trypsinization and then re-seeded in 96-well cell culture plates (Corning, Cat#07-200-90) at a concentration of 800 cells/well in 100□L of growth medium and incubated overnight. On the second day, each well was supplemented with 100□L DMSO (control), PARG inhibitor, or PARGi + NRH (100□M). The treated cells were incubated for 5 days then stained with propidium iodide (PI) and Hoechst 33342 (Thermo Fisher Scientific, Cat# R37605). The cell number live and dead cells of each well was counted using the Celigo Image Cytometer (Nexcelom Bioscience) in triplicate.

Nikon Confocal PAR Foci Analysis

U2OS/LivePAR or ES-2/LivePAR cells were seeded in 100mm cell culture dishes with 10mL of growth medium. At 80% confluency, cells were isolated by trypsinization and then re-seeded in 10mm cell culture dishes at a concentration of 250,000 cells/dish in 4mL of growth medium with a pre-treated cover slide and incubated overnight at 37°C with 5% CO2. After 20-24 hours, cells were treated with PARGi (PDD00017273; 10μM) and/or, PARPi (ABT-888; 10μM, Selleckchem, Cat# S1004), NRH (NuChem), MNNG (Sigma-Aldrich, Cat# 129941) and incubated at 37°C with 5% CO2 for 60 minutes. After incubation, the cells were washed three times with 1x PBS. Then, cells were pre-fixed with 4% formaldehyde, washed three times with 1x with PBS and fixed with cold 7:3 methanol:acetone (Fisher Scientific, Cat# A18-1, Cat# A452SK-4). Finally, the cells were washed a final time three times with 1x PBS. The cover slide was then mounted on a glass slide with Vectashield plus antifade mounting medium (Fischer

Scientific, Cat# NC1695563) with DAPI (Thermo Fisher Scientific, Cat# R37606). Cells were imaged using a Nikon A1rsi laser scanning confocal microscope. Image analysis using ImageJ was used to quantify PAR foci EGFP tag per cell nucleus (cite PMID# 40403420).

Opera Phenix 96-well Confocal PAR Foci Analysis

U2OS/LivePAR cells were seeded in 100mm cell culture dishes with 10mL of growth medium. At 80% confluency, cells were isolated by trypsinization and then re-seeded in a 96-well Revvity PhenoPlate (Cat# 6055302) at a concentration of 65,000 cells per well with 100µL of growth medium. Cells were incubated overnight at 37°C with 5% CO2. After 20-24 hours, cells were treated with PARGi (10µM) and/or, PARPi (10µM), NRH (100µM), MNNG (10µM), MMS (10µM), tBuOOH (40µM) and incubated for 60 minutes at 37°C with 5% CO2. After incubation, the cells were washed three times with 1x PBS and pre-fixed with 4% formaldehyde. The cells were then fixed with cold 7:3 methanol:acetone and washed two times with 1x PBS. PBS with DAPI (100µL) was finally added to the plate. Cells were imaged using an Opera Phenix Confocal microscope using water lens 30x.

Statistical Analysis

Most analyses of data are shown as the mean ± standard error of the mean (SEM). Means were calculated from multiple replicate experiments using three-parameter nonlinear regression, fitting data to sigmoidal models for significant differences. Exclusion criteria were used for foci count per cell nucleus with relative peak intensity below 1.15 were excluded from the experiment and statistical analysis. All statistical analyses were performed using GraphPad Prism 8 with P-values $p<0.05$.

Chapter 3: Results

Commented [4]: Everything in your results section should be publication quality

Figures should have appropriate legends and should be referenced in the text

You should have statistical analysis (sample size, P value when reporting something changed. etc.

3.1 Varying potency of PARGi and enhanced sensitivity of ES-2/XRCC1-deficent cells

To evaluate the potency of different PARGi inhibitors, ES-2 WT cells and ES-2 XRCC1 KO cells were treated with a panel of commercially available PARGi: PDD00017273, PDD000172738, PDD00017272, or JA2131. Cell viability was assessed following five days of incubation after treatment using PI and Hoechst staining.

Treatment of PARGi resulted in a decrease in cell viability in the ES-2/XRCC1-KO cells compared to the ES-2 WT cells and DMSO controls when treated with PDD00017273, PDD000172738, PDD00017272. However, a minimal decrease in variability was observed in all cells treated with JA2131(Figure 1C). The most potent PARGi was PDD00017272 with a less than 10% cell survival rate at the 1µM dose and 0% survival at 2µM dose and upwards (Figure1A). PDD00017273 was the next potent inhibitor with about a 5% survival rate at the 5µM dose (Figure 1B). PDD00017273 was mostly used in following experiments because it demonstrated strong and reproducible effects while maintain a suitable dynamic range for evaluating combination treatments and PAR foci quantification analysis. PDD000172738 (Figure 1D) showed around a 10% viability at the 5µM dose and finally, JA2131 only showed about 10-15% cell death at the 5µM dose. With all four inhibitors, the ES-2 WT cells showed minimum cell death when treated with PDD00017273, PDD000172738, and JA2131 (80% viability or higher). PDD00017272 showed the most percent cell death in ES-2 WT with around 90% killing at the 5µM dose.

Figure 1: ES-2 WT and ES-2 XRCC1 KO cells 96-well cell viability assay treated with PDD00017273, PDD000172738, PDD00017272, and JA2131. DMSO and cell media were used as controls.

Figure 1A

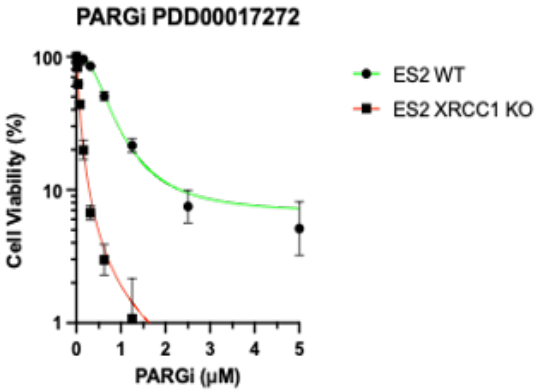

Figure 1B

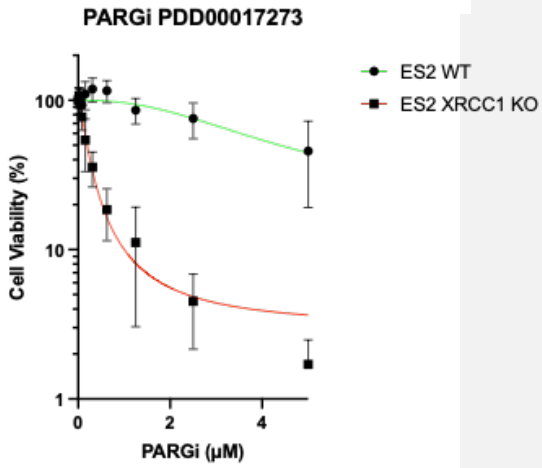

Figure 1C

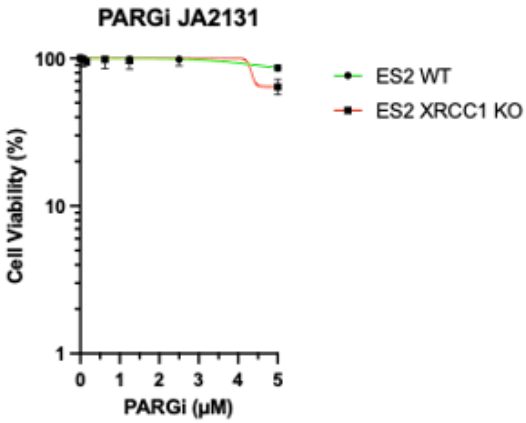

Figure 1D

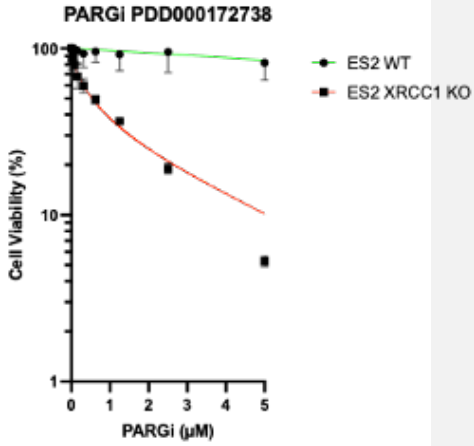

3.2 Differential sensitivity of an ovarian cancer cell line panel to PARGi and NRH co-treatment

To evaluate the impact and sensitivity of PARGi on ovarian cancer cell survival, a panel of ovarian cancer cell lines (ES-2, PA-1, COV362, RMUGS, SKOV-3, and OVTOKO) was treated with PARGi PDD00017273 in the presence or absence of NRH. Cell viability was assessed after cells were treated and incubated for five days following treatment. Live and dead cell counts were obtained using cell staining with PI and Hoechst dye.

Treatment with PARGi alone resulted in varying sensitivity across multiple ovarian cancer cell lines compared to controls. The most resistant cell lines were ES-2 cells with no impact on cell viability following treatment (Figure 2E). SK-OV-3 and OVTOKO WT cells showed little to no impact on viability when treated with the PARGi alone.(Figure 2A, Figure 2C). RMUGS, COV-362 and PA-1 cells showed the more sensitivity to PARGi, with ~30% or more cell viability

(Figure 2F, Figure 2B, Figure 2D). Notably, co-treatment with NRH further enhanced the reduction in cel survival in most cell lines. Specifically, co-treatment with NRH and PARGi resulted in less than 10% viability in the PA-1 cell line (Figure 2D). COV-362 cells showed some killing at around 30% while, SK-OV-3 and RMUGS cells all show about 70-80% killing at the 5µM dose (Figure 2B, Figure 2F). ES-2 cells were not very sensitive to PARGi and NRH with about 95% cells remaining viable (Figure 2E). Finally, OVTOKO cells showed no difference in cell viability after co-treatment with PARGi and NRH (Figure 2C). OVTOKO cells had similar viability after five days with less than 20% cell death (Figure 2C). These findings indicate that PARG inhibition may disrupt ovarian cancer cell survival in some cell lines and that NRH supplementation may enhance therapeutic response. Different cell lines have varying sensitivity to PARGi inhibition alone and/or PARGi co-treatment with NRH.

Figure 2: ES-2, PA-1, COV362, RMUGS, SKOV-3, and OVTOKO 96-well cell viability assay treated with PDD00017273 in the presence or absence of NRH. DMSO and cell media were used as controls.

Figure 2A

Figure 2C

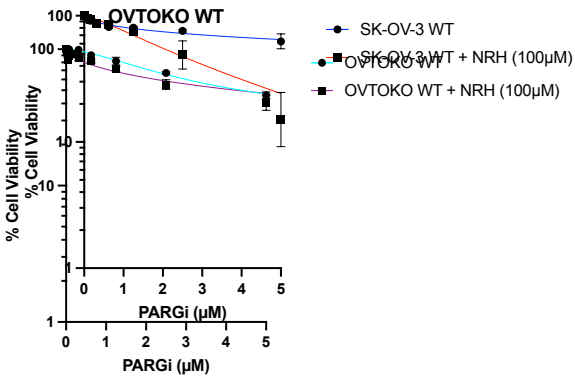

Figure 2B

Figure 2D

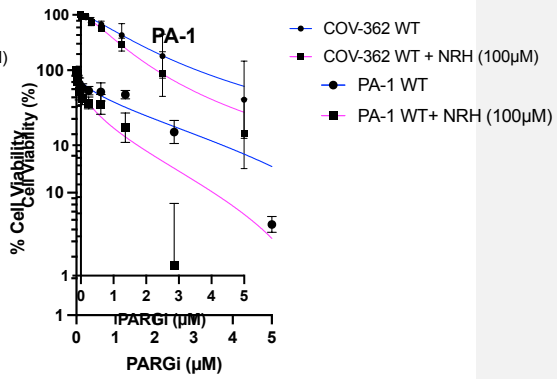

Figure 2E

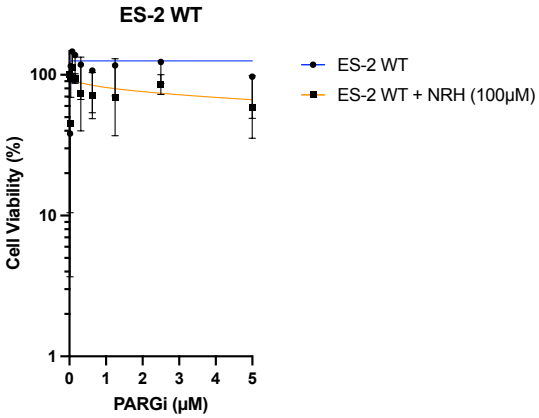

Figure 2F

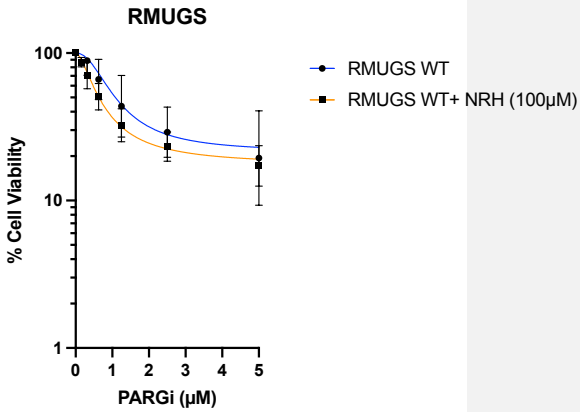

3.3. Effects of Combined PARGi, MNNG, and NRH Treatment on PAR Foci Formation in ES-2 Cell

To evaluate the moset effective combination of treatments for PAR foci in ES-2 Live/PAR cells, a combination of inhibitors, NRH and the genotoxin MNNG was used. ES-2 Live/PAR cells were treated with PARGi PDD00017273 (10μM) and/or PARPi Veliparib, ABT-888 (10μM) MNNG (10μM), and NRH (100μM). Cells were incubated for 60 minutes following treatment and PAR foci per nucleus per cell were analyzed using the A1rsi laser scanning confocal microscope. Image analysis was done using Image J with ~50 cells per image.

Overall, the combination treatment with the highest amount of PAR foci in ES-2 Live/PAR cells was PARGi, MNNG and NRH treatment when compared to controls and each treatment alone (Figure 3). The foci count collected was up to 60 PAR foci per cell (Figure 3). Secondly, MNNG

and PARGi treatment were sufficient to induce substantial PAR foci compared to controls; however, co-treatment with NRH seemed to show a further amplified effect (Figure 4). Addition of PARPi with PARGi, MNNG and/or NRH resulted in a reduction or no PAR foci formation, consistent with inhibition of PAR synthesis. Just PARGi, PARPi, NRH, or MNNG on their own did not have any significant increase in PAR foci with less than 20 PAR foci per cell per nucleus (Figure 3).

Figure 3

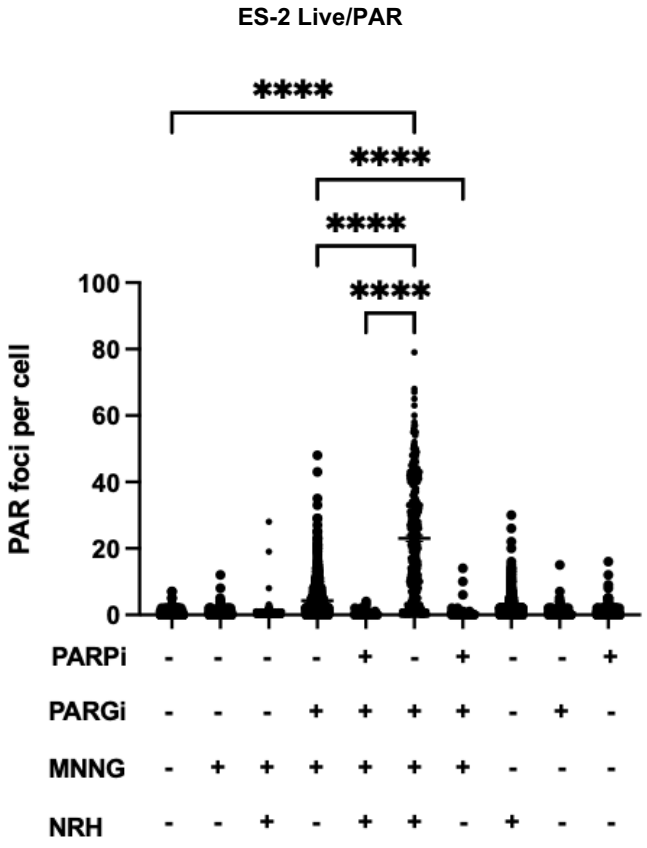

Figure 3: PAR foci count per cell in each treated condition in ES-2 Live/PAR cells using ImageJ analysis.

Figure 4: Nikon Confocal microscopy images of each treated condition and control groups (DMSO). MNNG, PARGi + NRH, and MNNG + PARGi groups showing visible foci within the nucleus.

Figure 4

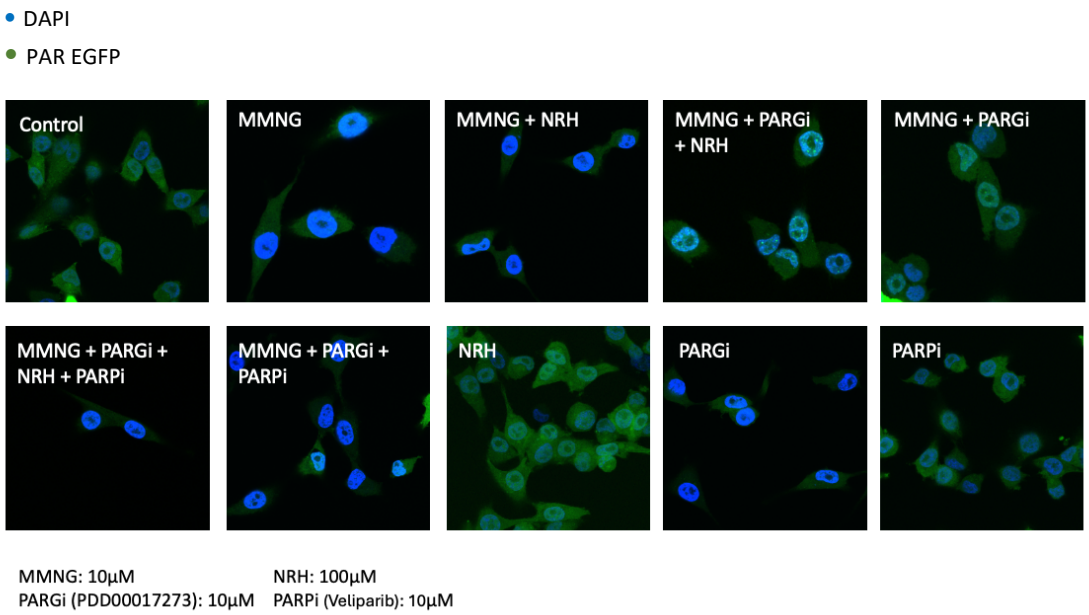

3.4 Differential PAR Foci Formation Induced by Genotoxins in U2OS Live/PAR Cells

To evaluate the effect of three genotoxins: MNNG, tBuOOH and MMS on PAR foci formation, U2OS Live/PAR cells were treated with each compound in a 96-well plate format (Figure 5a,

Figure 5b) Following treatment, cells were imaged using the Opera Phenix confocal system and PAR foci per nucleus per cell were quantified across multiple wells and treatments. Analysis was performed using Opera Phenix automated image analysis and ImageJ. Baseline control conditions showed minimum PAR foci formation, as well as low basal PAR activity in untreated cells.

Among the genotoxins tested, MNNG treatment resulted in the greatest increase in PAR foci formation. Cells that were treated with MNNG displayed substantial PAR foci compared to controls, with the highest co-treatments suggesting MNNG and PARGi combinations showing the highest increase relative to MMS and tBuOOH in U2OS Live/PAR cells (Figure 5b, Figure 7).

In contrast, treatment with tBuOOH resulted in a slight increase in PAR foci formation compared to controls. This increase was seen in the tBuOOH, NRH and PARGi co-treatment condition (Figure 7). All other conditions did not seem to have a significant impact on increasing or decreasing PAR foci when compared to media alone. Similarly, MMS treatment produced a slightly increase in PAR foci formation compared to media alone in the MMS and NRH, and MMS, NRH and PARGi treatments. However, MMS had an overall lower level compared to MNNG-induced PAR formation. (Figure 7).

Overall, these results demonstrated that different genotoxic agents induce varying levels of PAR foci formation in U2OS Live/PAR cells. Specifically, MNNG produces the strongest response in PAR foci formation per nucleus. Treatment with tBuOOH and MMS showed a minimum

increase in PAR foci formation. These findings indicate that alkylating damage induced by MNNG leads to robust PAR foci formation, whereas oxidative stress from tBuOOH and methylating stress from MMS have a decreased effect on PAR accumulation.

Figure 5a: Plate map and generated corresponding heat map of PAR foci from Opera Phenix confocal microscope. Figure 5b: Opera Phenix generated graph of each PAR foci count per cell, per well

Figure 5a

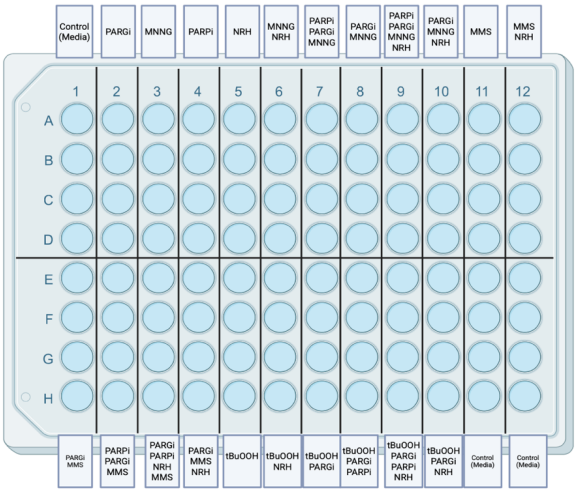

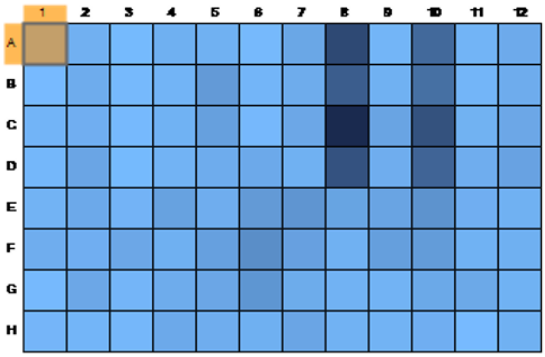

Heatmap: darker blue = higher foci

Figure 5b

U2OS Live/PAR

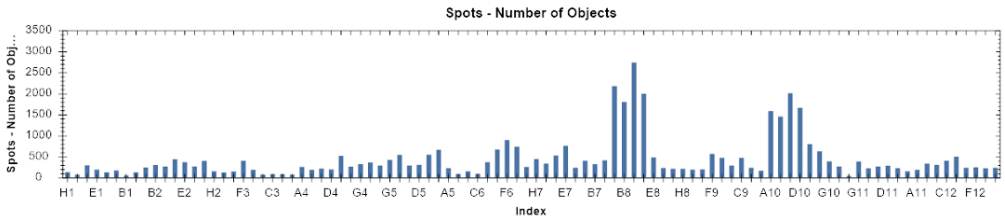

At 40x magnification water lens
Seeded 65k cells/per well

Figure 6: Confocal microscopy panels showing DAPI + EGFP, Control panel and PARGi, NRH, MNNG channel. PARGi, NRH, MNNG treatment shows visible PAR foci within the nucleus while control is clear.

Figure 6

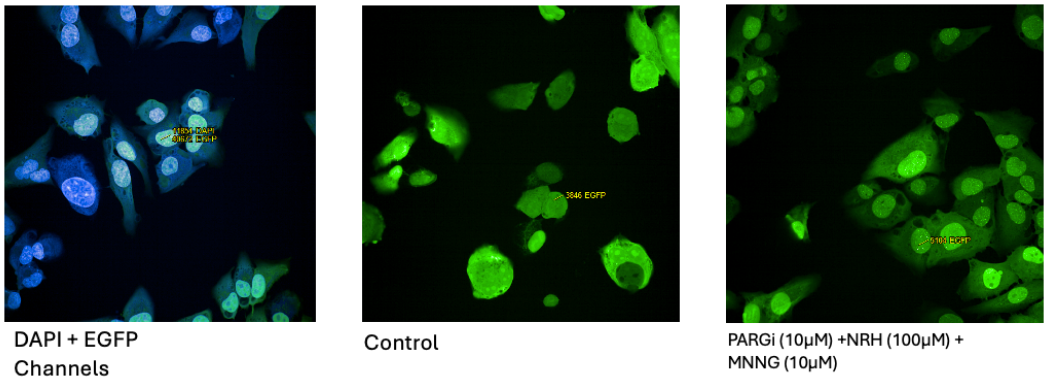

Figure 7: Graph depicting total PAR foci per well, per cell nucleus within each treated condition. Green shows MNNG treated condition, blue shows MMS treated condition and pink shows tBuOOH treated condition.

Figure 7

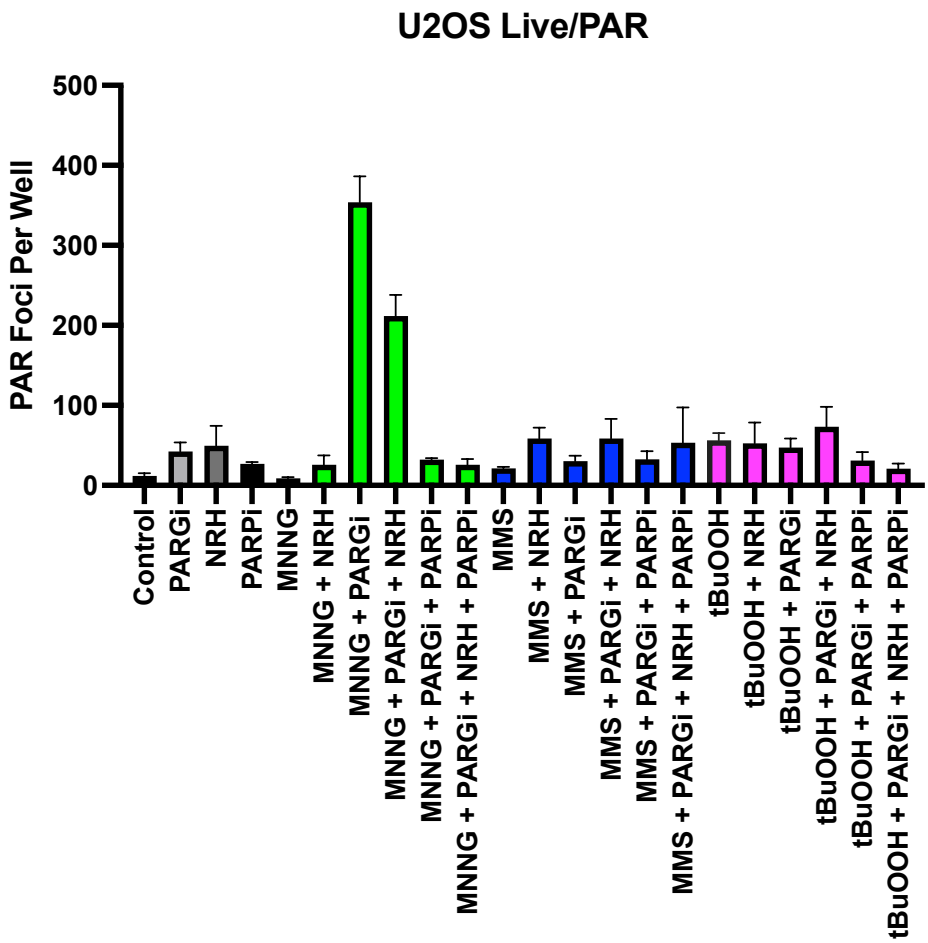

Chapter 4: Discussion

4.1 PARG Inhibitor Sensitivity in XRCC1-Deficient Ovarian Cancer Cells

In this study, ES-2 cells and ES-2/XRCC1-deficient cells were treated with a panel of different PARG inhibitors. ES-2/XRCC1-deficient cells demonstrated increased sensitivity to PARG inhibition compared to ES-2 wild-type cells. Treatment with PARG inhibitors PDD00017273, PDD000172738, and PDD00017272 resulted in a significant reduction in cell viability in the XRCC1 knockout cells, and minimal effects were observed in wild-type cells. The results suggest that an XRCC1 deficiency enhances sensitivity to PARG inhibition, which highlights a potential relationship between XRCC1 loss and PARG inhibition.

XRCC1 is a critical scaffold protein and plays a role in the single-strand break and base excision repair pathways [12,13]. These pathways repair DNA damage, such as chemically modified bases from radiation, toxins, or normal cellular metabolism. XRCC1 physically binds to DNA polymerase β, DNA ligase III, and PARP1 and stabilizes them during DNA damage [13]. Loss of XRCC1 impairs efficient stability in the recruitment of these enzymes, leading to increased reliance on other repair pathways [13]. Additionally, XRCC1 regulates PARP1 to prevent trapping [13]. If PARP1 stays bound to DNA for too long, PAR chain formation accumulates and can become a toxic physical block, as well as consuming large amounts of cellular NAD^+ [14]. Therefore, XRCC1-deficient cells may further exacerbate PAR chain accumulation, especially with the addition of PARG inhibition.

Interestingly, ES-2 cells are relatively resistant to PARG inhibition alone. This result suggests that other intact DNA repair mechanisms may protect cells from PARG inhibition-induced stress. ES-2 cells are also relatively resistant to PARP inhibition because they are homologous recombination repair (HRR) proficient as well as wild type for BRCA1/2 [15,16]. Likely, these cells are able to rely on HRR pathways to fix DNA damage, whereas deficient cells have fewer options for recovery. Investigating additional DNA repair-deficient models and combination therapies may help to best target patient populations that will benefit the most from PARG inhibitor treatment.

4.2 NRH Enhances PARGi-Induced Cytotoxicity

In this study, a panel of ovarian cancer cell lines was used to demonstrate varying sensitivity to PARG inhibition, with PA-1, COV362, and RMUGS cells showing the greatest reduction in viability and the highest sensitivity to PARG inhibition. ES-2, SKOV-3, and OVTOKO cells displayed minimal response to PARG inhibition alone. Additionally, all cells were also treated with a co-treatment of PARGi and NRH. Our findings show that the combination treatment with PARGi and NRH showed a varying decrease in cell viability.

Mechanistically, NRH is a precursor of NAD+, which can increase cellular NAD+ pools [17] (explain how). An increase in bioavailability of NAD+ provides sufficient substrate to fuel PARP1 activation [20]. PARP1 acts as a molecular sensor that coordinates DNA damage cellular response and acts as a scaffold builder using NAD+ to build long chains of PAR as well as recruit other essential repair proteins to sites of damage [21]. Adding NRH increases

accumulation of PAR, particularly during the S-phase cycle and creates replication stress by stalling replication forks [22, 52]. Adding a PARG inhibitor, in combination with NRH, further causes hyper-accumulation of PAR. PARG is the primary enzyme responsible for the degradation of PAR chains as well as regulating the release of PARP1 [22].

Furthermore, repair proficient cell lines like ES-2 and SKOV-3 displayed minimal response to PARGi alone but showed a slight increase in cell death when NRH was added. This shows that increasing NAD+ bioavailability may overwhelm inherent DNA repair capacity to some extent [23]. Furthermore, previous studies on OVTOKO showed high resistance to other PARP inhibitors, including talazoparib (BMN-673). For example, when OVTOKO is treated with a PARP inhibitor, other pathways like PI3K/AKT and CRY1 are activated [24]. Likely. OVTOKO utilizes other signaling pathways to protect replication forks [24]. Interestingly, COV-362 observed some killing but was not extremely sensitive to PARGi treatment. Although COV-362 is a BRCA1-deficient cell line, other mechanisms could be used to activate and maintain some survival when treated with PARGi alone [25, 51].

The two cell lines that were most sensitive to PARG inhibition alone were PA-1 and RMUGS, with PA-1 showing the greatest sensitivity when treated with a combination of NRH and PARGi. Although RMUGS is BRCA1/2 wild type, it is highly PARGi sensitive, suggesting that HR positivity on its own does not 100% guarantee resistance to PARG inhibition. Another study by Ravindranathan et al. suggests that RMUGS has inherent difficulties with Okazaki fragment processing on the lagging strand during DNA replication [25]. Thus, increasing PARylation may play a role in why RMUGS is sensitive to PARGi, as was suggested by Li et al (PMID #

34806016). Finally, PA-1 is known to be a highly sensitive cell line in general. PA-1 is highly sensitive to radiation treatments as well as various chemotherapies and small molecules [26, 27, 28]. Unlike the other cell lines, PA-1 is an ovarian teratocarcinoma (germ cell tumor) which naturally has a lower threshold for triggering apoptosis to prevent passing on mutations to offspring [29]. Additionally, PA-1 is p53 wild type, so PARGi treatment, which causes replication stress, would likely immediately trigger cell death [28], suggesting the possibility that PAR-induced S-phase arrest may depend, at least in part, on p53-mediated apoptosis.

In summary, this study demonstrated that ovarian cancer cell lines exhibit a wide variety of sensitivity to PARG inhibition. The introduction of the NAD+ precursor NRH also significantly increases cytotoxicity in most cell lines. Our results indicated that PARGi sensitivity may not predominantly depend on HR-positive or HR-negative cells and may be a consequence of the cell's ability to utilize other mechanisms or their inherent ability to manage replication-associated stress.

4.3 PAR Foci Formation in ES-2 Live/PAR Cells

In this study, ES-2/LivePAR cells were treated with multiple combinations of PARGi, PARPi, NRH and MNNG. Our results showed that the combination of MNNG, NRH and PARGi produced a three-fold increase (up to ~60) in PAR foci per cell compared to individual treatments (up to ~20 foci per cell). This suggest that maximum PAR accumulation requires simultaneous presence of a DNA damage signal, the metabolic substrate (NAD+), and inhibition of PAR degradation. While the combination of MNNG and PARGi alone provides sufficient

signal to visualize PAR foci, the addition of a metabolic precursor (NAD+) significantly amplifies this effect.

A critical limiting factor that involves PARylation (formation of PAR chains) is the availability of the substrate NAD+. PARP enzymes hydrolyze NAD+ and polymerizes ADP-ribose units onto target proteins. We observed that supplementing with NRH, which is an NAD+ precursor, rapidly increases NAD+ levels [30, 31]. Thus, co-treatment with NRH provides the “fuel” to form larger and longer PAR chains. MNNG is an alkylating agent which attaches an alkyl group to DNA and creates the substrates for the BER pathway [32] that leads to an increased level of DNA breaks as intermediates in DNA repair. These breaks serve as co-factors that switch PARP1 from an inactive state to active state [32]. It is likely the synergy between overactivation of PARP1 and high NAD+ levels that allows for high accumulation of PAR chains. PARGi is the final component of synergy which allows for elevated levels of PAR foci. PARG acts as the “eraser” to degrade PAR chains almost as quickly as they are synthesized; thus, to visualize PAR dynamics, inhibiting PAR degradation is crucial [30].

Additionally, combination treatment with NRH, MNNG, PARGi and PARPi (Veliparib) or MNNG, PARGi and PARPi blocks PAR foci formation. Inhibiting PARP1 blocks its catalytic activity, preventing PARylation what would normally be detected as foci [36]. As highlighted by Paradkar et al. [53], the formation of visible nuclear aggregates or 'foci' is structurally dependent on the synthesis of these PAR polymers. By introducing a PARPi, PARP1 cannot synthesize PAR chains detectable by confocal microscopy. PARPi effectively 'mutes' the cellular PARylation response, ensuring that even under high-stress conditions, such as MNNG treatment, the LivePAR sensor remains unable to detect any localized signal accumulation.

Ultimately, the observed peak of ~60 PAR foci represent a critical transition from a manageable DNA damage response to a state of elevated PARylation. By simultaneously maximizing the damage signal with MNNG, providing a metabolic fuel source via NRH, and preventing enzymatic recovery with PARGi, we have successfully 'locked' the ES-2 cells into a state of genomic and metabolic exhaustion. This synergy demonstrates that while these cells may possess robust repair mechanisms, they can be sensitized to cell death by strategically overwhelming the PAR cycle beyond its physiological recovery limit.

4.4 Genotoxin-Dependent PAR Foci Formation in U2OS Live/PAR Cells

The main finding of this study showed significant differences in various known genotoxins on PAR foci accumulation. In U2OS/LivePAR cells, MNNG was the most potent inducer of PARylation and consistently outperformed PAR formation from oxidative stress induced by tBuOOH or methylating stress induced by MMS. MNNG treatment was found to trigger robust, high-density formation of nuclear PAR foci, compared to controls, which exhibited minimal PAR activity. This finding shows that in LivePAR quantification tracking systems, the PARP1 enzymatic machinery may be specifically tuned to DNA lesions produced by MNNG or that the MNNG doses used produced an increased level of DNA lesions. These lesions may serve as high-affinity recruitment signals for PARP1 activation during base excision repair (BER).

In the previous study, NRH, MNNG and PARGi co-treatment resulted in maximized PAR foci quantification as measured by confocal microscopy. Because tBuOOH and MMS failed to reach

similar levels of PAR foci, as compared to MNNG, NRH supplementation and NAD+ bioavailability was not a limiting factor.

MMS is a methylating agent which converts guanine to 7-methylguanine and adenine to 3-methyladenine [33]. In previous studies, MMS is used as a classical BER specific genotoxin. MMS did not cause any double stranded DNA breaks (DSBs) in animal models, but did show MMS-induced stalled replication forks, only in high heat temperatures [33]. PARP1, as well as PARP2, are normally “nick sensors” and activates when they physically encounter a DNA strand break such as single strand breaks (SSB), or DSBs. In this study. we treated U2OS/LivePAR cells for 60 minutes so perhaps a longer incubation time or higher dose of MMS may induce sufficient DSBs or SSBs to activate PARP1 and PARP2 to accumulate PAR foci.

Finally, tBuOOH treatment also showed minimum accumulation of PAR foci, even when supplemented with NRH and the PARGi. tBuOOH is a genotoxin that mediates DNA damage through oxidation, specifically creating oxidative base modifications like 8-hydroxyguanine and thymine glycol. These are relatively stable lesions which require enzymatic processing via BER [35]. In previous studies, tBuOOH was shown to be a potent inducer of ferroptosis, which is an iron-dependent regulated apoptosis [34]. They found that tBuOOH can cause DSBs and replication blocks independently of nuclear damage [34]. It is likely that the doses used of tBuOOH in this study were simply too low to generate sufficient DNA damage to activate PARP1 and/or PARP2.

In summary, these results establish that the robust quantification of PAR foci is dependent on a specific threshold of DNA strand-break density that is uniquely provided by MNNG-induced alkylation at the doses used. While NRH and PARGi are essential for amplifying and stabilizing the signal, they cannot always compensate for initial PARP1 recruitment. The minimal response observed with MMS and tBuOOH, is most likely the result of insufficient doses of the agents to induced PARP1 activation. This identifies MNNG at the doses use as the optimal tool for validating PAR-tracking probes and studying the maximal capacity of the cellular PARylation machinery.

Chapter 5: Conclusion

In conclusion, this study investigates the therapeutic potential of PARG inhibition on ovarian cancer as well as its effects on DNA damage and repair capacity, genomic stress, and metabolic substrate availability. Overall findings show that resistant cells like ES-2 and SK-OV-3 exhibit inherent resistance to PARG inhibition on their own. However, such resistances can be overcome through addition of a NAD+ precursor such as NRH which can move ovarian cancer cells towards a more lethal state of PAR-overload and metabolic exhaustion. Additionally, cell lines with deficiency of scaffolding proteins like XRCC1 can be strategically exploited as they show increased sensitivity to PARG inhibitors. Furthermore, quantifying conditions for PARylation through Live/PAR tools, help to better understand mechanisms that govern genomic repair and cellular exhaustion. Identifying synergy between DNA damage, metabolic fuelling and PAR

accumulation agents provides a framework for overcoming limitations of current PARP inhibitor therapies. Ultimately, these results suggest targeting a wider view of the PAR cycle rather than specific enzymes offer a viable strategy to bypass repair-proficient ovarian cancers and provide potential personalized therapeutic interventions.

Currently, treatment is often limited to patients with BRCA1/2 mutations; however, our data suggest that PARG inhibitors, particularly when combined with metabolic precursors like NRH, could expand the targetable patient population to include those with XRCC1 deficiencies or other non-HR repair defects. By transitioning from simple enzymatic inhibition to different combination strategies that maximize damage, metabolic activity, and stabilization, we can effectively bypass traditional resistance mechanisms and force even aggressive ovarian cancer subtypes to become more sensitive to different therapeutic treatments. While this study establishes a clear mechanistic link between PAR metabolism, DNA repair deficiency, and cytotoxicity in ovarian cancer, several avenues remain for future investigation and optimization.

References

1. Zhu H, Li JH, Zhan J, et al. PARP inhibitors in ovarian cancer: sensitive or resistant? *Front Oncol*. 2022;12:931327.
2. National Cancer Institute. SEER stat fact sheets: ovarian cancer. *SEER*. http://seer.cancer.gov/statfacts/html/ovary.html. Accessed 2024.
3. Acharya G, Mani C, Sah N, et al. CHK1 inhibitor induced PARylation by targeting PARG causes excessive replication and metabolic stress and overcomes chemoresistance in ovarian cancer. *Cell Death Discov*. 2024;10(1):278.
4. Li J, Koczor CA, Saville KM, et al. Overcoming Temozolomide Resistance in Glioblastoma via Enhanced NAD(+) Bioavailability and Inhibition of Poly-ADP-Ribose Glycohydrolase. *Cancers (Basel)*. 2022;14(15):3572.
5. Pillay N, Angelini RP, Itamochi H, et al. The landscape of HRD in ovarian cancer. *Cancers (Basel)*. 2021;13(22):5722.
6. Hoppe MM, Huynen L, Lopez-Garcia C, et al. Understanding PARP inhibitor resistance in ovarian cancer. *Int J Mol Sci*. 2024;25(24):13549.
7. Ngoi NY, Tan DS. The role of homologous recombination deficiency (HRD) as a predictive biomarker of response to PARP inhibitors in ovarian cancer. *Front Oncol*. 2021;11:692997.
8. Lheureux S, Gourley C, Vergote I, Oza AM. Epithelial ovarian cancer. *Lancet*. 2019;393(10177):1240-1253.
9. Zhu H, Zhan J, et al. (Repetitive entry of Acharya et al. or Zhu et al.). *Cell Death Discov*. 2024;10(1):278.

10. Li H, Liu ZY, Wu N, et al. PARP inhibitor resistance: the underlying mechanisms and clinical implications. *Mol Cancer*. 2020;19:107.
11. Kim D, Nam HJ. PARP inhibitors: clinical limitations and recent attempts to overcome them. *Int J Mol Sci*. 2022;23:8412.
12. Caldecott KW. Single-strand break repair and genetic disease. *Nature Reviews Genetics*. 2008;9:619–631.
13. Demin AA, Hirota K, Tsuda M, et al. XRCC1 prevents toxic PARP1 trapping and DNA double-strand breaks at damaged replication forks. *Nat Commun*. 2021;12:3109.
14. Rose M, Burgess JT, O'Byrne K, et al. PARP Inhibitors: Clinical Relevance, Mechanisms of Resistance and Future Prospects. *Front Oncol*. 2020;10:1285.
15. Slade D. PARP and PARG inhibitors in cancer treatment. *Chem Soc Rev*. 2020;49(14):360-380.
16. Hanzlikova H, Gittens W, Krejcikova K, et al. Overlapping roles for PARP1 and PARP2 in the recruitment of repair factors to DNA breaks. *Nucleic Acids Res*. 2020;48(12):6574-6588.
17. Navas LE, Carnero A. NAD+ metabolism, aging, and cancer. *Signal Transduct Target Ther*. 2021;6:371.
18. Fletcher SCR, et al. NAD+ metabolism in DNA repair and cancer cell survival. *Antioxid Redox Signal*. 2023;0354.
19. Canto C, Menzies KJ, Auwerx J. NAD+ Metabolism and the Control of Energy Homeostasis: A Balancing Act between Coenzyme and Sensor. *Endocr Rev*. 2015;36(6):646-689.

20. Li J, Sobol RW. The role of PARG in the cellular response to DNA damage. *DNA Repair*. 2024;1568.
21. Gibson BA, Kraus WL. New insights into the molecular and cellular functions of poly(ADP-ribose) and PARPs. *Nat Rev Mol Cell Biol*. 2012;13(7):411-424.
22. Barkauskas DA, et al. NAD+ salvage pathway in cancer. *PubMed*. 2013;23809438.
23. Ravindranathan R, et al. PARG inhibition as a strategy in ovarian cancer. *PMC*. 2024;10887177.
24. Murai J, Huang SY, Das BB, et al. Trapping of PARP1 and PARP2 by Clinical PARP Inhibitors. *Cancer Res*. 2012;72(21):5588-5599.
25. Ravindranathan R, et al. Okazaki fragment processing and PARG sensitivity. *PMC*. 2024;11588084.
26. Zeisig BB, et al. PA-1 cells and radiation sensitivity. *PMC*. 2022;8984132.
27. Monaghan P, et al. PA-1 chemotherapy sensitivity. *PubMed*. 2004;15487701.
28. Smith AD, et al. p53 status in PA-1 cell lines. *PubMed*. 2002;12469184.
29. Tainsky MA, et al. Differentiation and tumorigenicity of PA-1. *PubMed*. 1991;1681491.
30. Li J, et al. PARP and NAD+ dynamics. *DNA Repair*. 2025;000412.
31. Li J, et al. Overcoming Temozolomide Resistance. *Cancers (Basel)*. 2022;14:3572.
32. Chiu LY, et al. Oxidative stress initiates DNA damager MNNG-induced parthanatos. *Biochem Pharmacol*. 2011;81:459-470.
33. Lundin C, et al. MMS produces heat-labile DNA damage but no in vivo DSBs. *Nucleic Acids Res*. 2005;33(12):3799-3811.
34. Wenz C, et al. Cell-cell contacts protect against t-BuOOH-induced ferroptosis. *Arch Toxicol*. 2019;93:1265-1279.

35. Altman SA, et al. tert-Butyl hydroperoxide-mediated DNA base damage. *Mutat Res*. 1994;306:35-44.

36. Paradkar S, et al. PARG inhibition induces nuclear aggregation of PARylated PARP1. *Structure*. 2024;32:2083-2093.

37. Siegel RL, Miller KD, Fuchs HE, Jemal A. Cancer statistics, 2021. *CA Cancer J Clin*. 2021;71:7–33.

38. Damia G, Broggini M. Platinum resistance in ovarian cancer: role of DNA repair. *Cancers (Basel)*. 2019;11:119.

39. Rosenberg B, Vancamp L, Krigas T. Inhibition of cell division by platinum. *Nature*. 1965;205:698–9.

40. Kelland L. The resurgence of platinum-based cancer chemotherapy. *Nat Rev Cancer*. 2007;7:573–84.

41. Harrap K. Preclinical studies identifying carboplatin. *Cancer Treat Rev*. 1985;12:21–33.

42. Gibson BA, Kraus WL. New insights into molecular and cellular functions of PARP. *Nat Rev Mol Cell Biol*. 2012;13:411–424.

43. Gupte R, Liu Z, Kraus WL. PARPs and ADP-ribosylation. *Genes Dev*. 2017;31:101–126.

44. Ray Chaudhuri A, Nussenzweig A. The multifaceted roles of PARP1 in DNA repair. *Nat Rev Mol Cell Biol*. 2017;18:610–621.

45. Kassab MA, Yu X. The role of dePARylation in DNA damage repair. *DNA Repair (Amst)*. 2019;76:20–29.

46. Fisher AE, et al. Poly(ADP-ribose) polymerase 1 accelerates SSB repair. *Mol Cell Biol*. 2007;27:5597–5605.

47. Ray Chaudhuri A, et al. PARG prevents accumulation of replication structures. *Mol Cell Biol*. 2015;35:856–865.

48. Dias, M.P., Moser, S.C., Ganesan, S. et al. Understanding and overcoming resistance to PARP inhibitors in cancer therapy. *Nat Rev Clin Oncol* 2021;18, 773–791.

49. Singh, Satyakam & Makwana, Dilip & Buckley, Terrisha & Agrawal, Arun & Koduru, Srinivas V & Tiwari, Amit. Clinical significance of PARP-1 inhibitors in cancer chemotherapy. *Translational Clinical Biology.* 2013;1. 10-15.

50. Albitar M, Zhang H, Pecora A, et al. Homologous Recombination Abnormalities Associated With BRCA1/2 Mutations as Predicted by Machine Learning of Targeted Next-Generation Sequencing Data. *Breast Cancer (Auckl).* 2023;17:11782234231198979.

51. Nesic K, Krais JJ, Vandenberg CJ, et al. BRCA1 secondary splice-site mutations drive exon-skipping and PARP inhibitor resistance. Preprint. medRxiv. 2023

52. Li J, M Saville K, Ibrahim M, Zeng X, McClellan S, Angajala A, Beiser A, Andrews JF, Sun M, Koczor CA, Clark J, Hayat F, Makarov MV, Wilk A, Yates NA, Migaud ME, Sobol RW. NAD+ bioavailability mediates PARG inhibition-induced replication arrest, intra S-phase checkpoint and apoptosis in glioma stem cells. *NAR Cancer*. 2021

53. Paradkar, Sateja et al. PARG inhibition induces nuclear aggregation of PARylated PARP1. *Structure (London, England : 1993) vol. 32,11*. 2024; 2083-2093.

Supplemental Figures

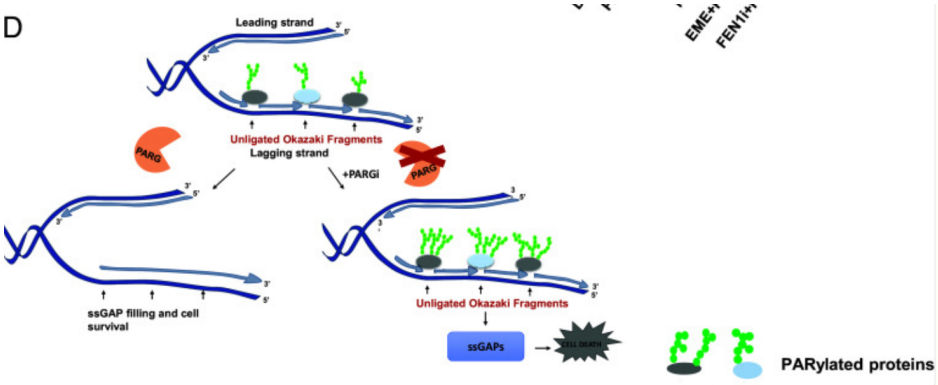

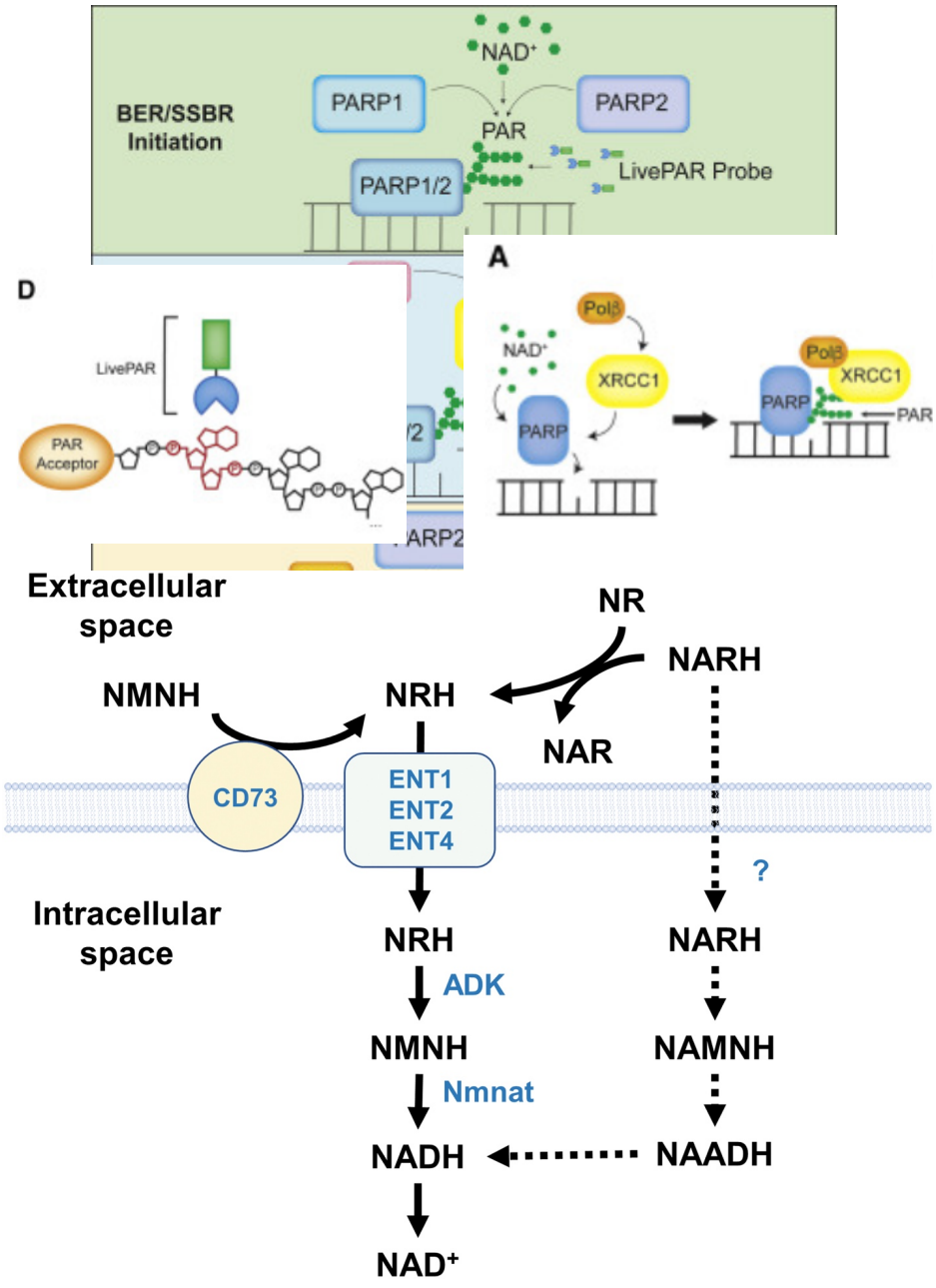
BER/SSBR
Initiation
NAD+
PARP1
PARP2
PAR
PARP1/2
LivePAR Probe
D
LivePAR
PAR
Acceptor
A
Polβ
NAD+
XRCC1
PARP
PAR
Extracellular
space
NR
NARH
NMNH
NRH
NAR
CD73
ENT1
ENT2
ENT4
?
Intracellular
space
NRH
NARH
ADK
NMNH
NAMNH
Nmnat
NADH
NAADH
NAD+

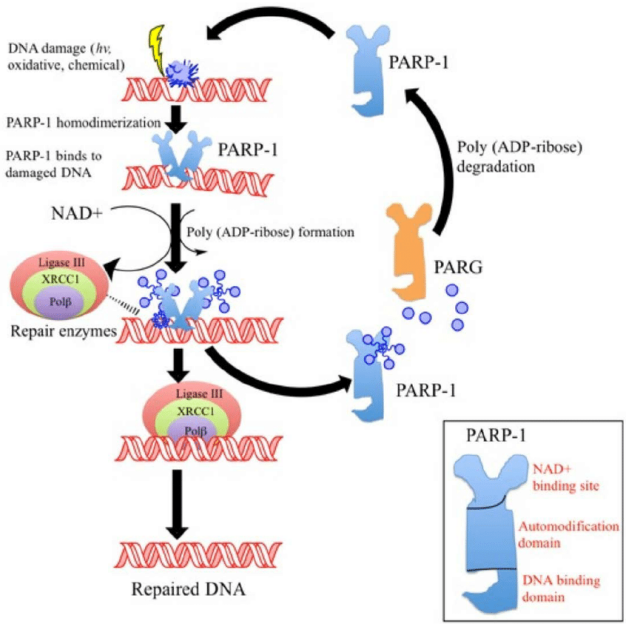
DNA damage (hv, oxidative, chemical)
PARP-1 homodimerization
PARP-1 binds to damaged DNA
PARP-1
NAD+
Poly (ADP-ribose) formation
Ligase III
XRCC1
Polβ
Repair enzymes
Ligase III
XRCC1
Polβ
Repaired DNA
PARP-1
Poly (ADP-ribose) degradation
PARG
PARP-1
PARP-1
NAD+ binding site
Automodification domain
DNA binding domain